**Atmospheric
Chemistry
and Physics**
Discussions

Open Access

Non-OH chemistry in oxidation flow reactors for the study of atmospheric chemistry systematically examined by modeling

Z. Peng[1,2], D. A. Day[1,2], A. M. Ortega[1,3,a], B. B. Palm[1,2], W. W. Hu[1,2], H. Stark[1,2,5], R. Li[1,3,4,b], K. Tsigaridis[6,7], W. H. Brune[8], and J. L. Jimenez[1,2]

[1]Cooperative Institute for Research in Environmental Sciences, University of Colorado, Boulder, CO 80309, USA
[2]Department of Chemistry and Biochemistry, University of Colorado, Boulder, CO 80309, USA
[3]Department of Atmospheric and Oceanic Sciences, University of Colorado, Boulder, CO 80309, USA
[4]Chemical Sciences Division, Earth System Research Laboratory, National Oceanic and Atmospheric Administration, Boulder, CO 80305, USA
[5]Aerodyne Research, Inc., Billerica, MA 01821, USA
[6]Center for Climate Systems Research, Columbia University, New York, NY 10025, USA
[7]NASA Goddard Institute for Space Studies, New York, NY 10025, USA
[8]Department of Meteorology, Pennsylvania State University, University Park, PA 16802, USA

Discussion Paper | Discussion Paper | Discussion Paper | Discussion Paper |

ACPD

15, 23543–23586, 2015

Non-OH chemistry in oxidation flow reactors

Z. Peng et al.

Title Page

Abstract	Introduction
Conclusions	References
Tables	Figures

|◀ ▶|

◀ ▶

Back Close

Full Screen / Esc

Printer-friendly Version

Interactive Discussion

[a]now at: Chemical and Environmental Engineering, University of Arizona, Tucson, AZ 85721, USA

[b]now at: Markes International, Inc., Cincinnati, OH 45242, USA

Correspondence to: J. L. Jimenez (jose.jimenez@colorado.edu)

ACPD

15, 23543–23586, 2015

Non-OH chemistry in oxidation flow reactors

Z. Peng et al.

Title Page

Abstract	Introduction
Conclusions	References
Tables	Figures

|◀ ▶|

◀ ▶

Back Close

Full Screen / Esc

Printer-friendly Version

Interactive Discussion

Abstract

Oxidation flow reactors (OFRs) using low-pressure Hg lamp emission at 185 and 254 nm produce OH radicals efficiently and are widely used in atmospheric chemistry and other fields. However, knowledge of detailed OFR chemistry is limited, allowing
5   speculation in the literature about whether some non-OH reactants, including several not relevant for tropospheric chemistry, may play an important role in these OFRs. These non-OH reactants are UV radiation, $O(^1D)$, $O(^3P)$, and O_3. In this study, we investigate the relative importance of other reactants to OH for the fate of reactant species in OFR under a wide range of conditions via box modeling. The relative impor-
10   tance of non-OH species is less sensitive to UV light intensity than to relative humidity (RH) and external OH reactivity (OHR_{ext}), as both non-OH reactants and OH scale roughly proportional to UV intensity. We show that for field studies in forested regions and also the urban area of Los Angeles, reactants of atmospheric interest are predominantly consumed by OH. We find that $O(^1D)$, $O(^3P)$, and O_3 have relative contributions
15   to VOC consumption that are similar or lower than in the troposphere. The impact of O atoms can be neglected under most conditions in both OFR and troposphere. Under "pathological OFR conditions" of low RH and/or high OHR_{ext}, the importance of non-OH reactants is enhanced because OH is suppressed. Some biogenics can have substantial destructions by O_3, and photolysis at non-tropospheric wavelengths (185
20   and 254 nm) may also play a significant role in the degradation of some aromatics under pathological conditions. Working under low O_2 with the OFR185 mode allows OH to completely dominate over O_3 reactions even for the biogenic species most reactive with O_3. Non-tropospheric VOC photolysis may have been a problem in some laboratory and source studies, but can be avoided or lessened in future studies by diluting
25   source emissions and working at lower precursor concentrations in lab studies, and by humidification. SOA photolysis is shown to be insignificant for most functional groups, except for nitrates and especially aromatics, which may be photolyzed at high UV flux settings. Our work further establishes the OFR's usefulness as a tool to study atmo-

Title Page

Abstract	Introduction
Conclusions	References
Tables	Figures

|◄   ►|

◄   ►

Back   Close

Full Screen / Esc

Printer-friendly Version

Interactive Discussion

Discussion Paper | Discussion Paper | Discussion Paper | Discussion Paper

spheric chemistry and enables better experiment design and interpretation, as well as improved future reactor design.

1 Introduction

For decades, environmental chambers have been employed to study atmospheric chemical processes, particularly, volatile organic compound (VOC) oxidation processes in the atmosphere (Cocker et al., 2001; Carter et al., 2005; Presto et al., 2005; Wang et al., 2011; Platt et al., 2013), without the interference of some transport processes (e.g., advection and wet deposition). These oxidation processes are the key to secondary organic aerosol (SOA) formation (Odum et al., 1996; Hoffmann et al., 1997; Hallquist et al., 2009), and air pollutant removal (Levy II., 1971). Atmospheric simulation chambers usually have volumes on the order of several m^3, and use light sources longer than 300 nm (e.g., sunlight or UV blacklights) to generate oxidants (mainly OH). These settings leads to OH concentrations (10^6–10^8 molecules cm^{-3}) that are not much higher than the typical ambient values (10^6–10^7 molecules cm^{-3}; Mao et al., 2009). Relatively low OH concentrations require long residence/simulation times (generally hours) and limit the ability of those setups to reach very high photochemical ages that are atmospherically-relevant (George et al., 2007; Kang et al., 2007; Carlton et al., 2009; Seakins, 2010; Wang et al., 2011). Residence times are ultimately limited due to losses of gases and particles to Teflon walls with timescales of tens of minutes to several hours (Cocker et al., 2001; Matsunaga and Ziemann, 2010; Zhang et al., 2014) as well as by the limited volume of the bag relative to the sampling instrumentation (Nguyen et al., 2014). Besides, large sizes and support systems (e.g. clean air generators) make it difficult to use large chambers in field or source studies.

Oxidation flow reactors (OFR) are an alternative that offers some advantages over environmental chambers, especially for rapid changes of experimental conditions, and/or for field experiments. They generally have a smaller size (on the order of 10 L), and typically use low-pressure Hg lamps as light sources for producing OH in large

amounts via O_3 and/or H_2O photolysis. These design choices lead to good portability, short experimental timescales, ability to reach long photochemical ages, and potentially reduced wall losses.

Due to these advantages, OFRs have been employed in many recent field and labo-
5 ratory studies in atmospheric chemistry, particularly in SOA-related research (George et al., 2007; Kang et al., 2007, 2011; Smith et al., 2009; Massoli et al., 2010; Cubison et al., 2011; Lambe et al., 2011a, b, 2012, 2013; Bahreini et al., 2012; Saukko et al., 2012; Wang et al., 2012; Ortega et al., 2013; Li et al., 2013). OFRs are also used in related applied fields, such as scrubbing of pollution from air (Johnson et al., 2014). In
10 contrast to their popularity, the chemistry occurring in OFRs is still incompletely char-
acterized, although the formation and interconversion reactions of most oxidants in OFRs have been well characterized (Sander et al., 2011; Ammann et al., 2015). To our knowledge, there are only three studies of OFR radical oxidation chemistry up to date: Ono et al. (2014) focused on the dependence of O_3 destruction on H_2O concentration.
15 We have recently made progress on the characterization of HO_x radical chemistry in OFRs (Li et al., 2015; Peng et al., 2015). We have developed a kinetic model for OFRs, which provides predictions in good agreement with laboratory experiments. This model has also shown that OH exposure (OH_{exp}, i.e., OH concentration integrated over the reactor residence time) increases with H_2O concentration and UV intensity, and de-
20 creases with external OH reactivity [$OHR_{ext} = \sum k_i c_i$, i.e., the sum of the products of concentrations of externally introduced OH-consuming species (c_i) and rate constants of their reactions with OH (k_i)]. The OH_{exp} decrease due to OHR_{ext} was defined as "OH suppression," and can reach two orders-of-magnitude in some cases (Li et al., 2015; Peng et al., 2015). We also showed that relative uncertainties of the outputs of our box
25 model (e.g., OH_{exp}) due to uncertain kinetic parameters are typically only 20 % (Peng et al., 2015). However, none of these studies directly address the fate of VOCs, simply regarded as external OH reactants in the prior studies.

The primary reason for the use of the OFRs studied here is for the study of reactions of species or mixtures of atmospheric relevance with the OH radical. However, other

Title Page

Abstract | Introduction

Conclusions | References

Tables | Figures

◄ | ►

◄ | ►

Back | Close

Full Screen / Esc

Printer-friendly Version

Interactive Discussion

highly reactive species are also present at very elevated concentrations, including the radicals $O(^1D)$ and $O(^3P)$, 185 and 254 nm photons, and O_3. If a substantial fraction of the species of interest reacted with those non-OH reactants, then the chemistry in the OFR would deviate from the OH radical chemistry intended to investigate. The ab-
5   sence of systematic research on VOC fate in OFRs leaves room for some speculation that non-OH or non-tropospheric chemistry can play a major role in OFRs: for example, Johnson et al. (2014) suggested that $O(^1D)$ and $O(^3P)$ significantly consumed VOCs. Klems et al. (2015) concluded that photons at 254 nm from Hg-lamp emission played an important role in their OFR experiment, especially for downstream peroxy radical
10   chemistry. Lack of clarity about these types of questions and of clear guidelines about how to apply OFRs to avoid such problems have limited the application of OFRs for years. In this paper, we apply the model in Peng et al. (2015) to systematically investigate whether significant non-tropospheric or non-OH chemistry occurs in OFRs, and what experimental conditions make it more important. The results allow improved
15   OFR operation and experimental design, as well as guidance for the design of future reactors.

2   Methods

The OFR and the model used here have been described in detail elsewhere (Kang et al., 2007; Li et al., 2015; Peng et al., 2015). Here, we only present a brief introduction
20   for each.

2.1   Potential Aerosol Mass flow reactor

Kang et al. (2007) first introduced the Potential Aerosol Mass (PAM) flow reactor. Although there were earlier versions of the PAM reactor, the version of cylindrical geometry with a volume of ~ 13 L has been widely used and is currently in use in many SOA
25   research groups (Massoli et al., 2010; Cubison et al., 2011; Kang et al., 2011; Lambe

et al., 2011a, b, 2012, 2013; Bahreini et al., 2012; Saukko et al., 2012; Wang et al., 2012; Li et al., 2013; Ortega et al., 2013). The reactor is made of aluminum or of glass and aluminum, and equipped with 1–4 low-pressure Hg lamps (model no. 82-9304-03, BHK Inc.) located inside the flow tube. The Hg lamps produce UV emissions at 185 and
5 254 nm, whose intensity can be rapidly computer-controlled. The operation mode using both 185 and 254 nm emissions is called "OFR185". In this mode, photons at 185 nm dissociate H_2O and O_2 molecules to produce $OH + H$ and $O(^3P)$, respectively. Recombination of $O(^3P)$ with O_2 forms O_3. UV light at 254 nm then photolyzes O_3 to produce $O(^1D)$, which reacts with H_2O and produces additional OH. OFR can also be operated
10 in another mode where photons at 185 nm are filtered by quartz sleeves around the lamps. In this case, only 254 nm UV light is active to generate OH ("OFR254" mode), and injection of externally generated O_3 into the reactor is required for OH production. The amount of injected O_3 plays a critical role in the OFR chemistry (Peng et al., 2015). For this reason this amount (X ppm) is also included in OFR operation mode notation in
15 the form of OFR254-X. For example, OFR254-70 and OFR254-7 denote experiments with 70 and 7 ppm O_3 injected, respectively. We use the PAM as the basic OFR design. Other designs will be specified below if needed.

2.2 Model description

We use the same model as in Peng et al. (2015), a standard chemical-kinetic model un-
20 der plug-flow conditions. The effect of non-plug flow residence time distributions (RTD) was also investigated in that study. Non-plug-flow models result in similar OHexp than plug-flow in most cases, except under specific conditions with very high UV, H_2O, and OHR_{ext}. Therefore, plug-flow OHexp is used in this study, as a proxy of OH_{exp} estimated from OHR_{ext} decay and to avoid the much increased computational expense for
25 complex RTDs. All O_x and HO_x reactions available in the JPL Chemical Kinetic Data Evaluation (Sander et al., 2011) are taken into account. Reactions of some external OH reactants (externally introduced reactants destructing OH), such as SO_2, CO and

NO$_x$, are also included. SO$_2$ is used as a proxy of other external OH reactants (e.g., VOCs). We believe that this is a realistic approximation in terms of OHR$_{ext}$ decay vs. OH$_{exp}$, as discussed in Peng et al. (2015).

When studying the OFR, we assume a residence time of 180 s, and use typical temperature (295 K) and atmospheric pressure (835 mbar) in Boulder, CO, USA. H$_2$O mixing ratio (abbr. H$_2$O hereafter) ranges from 0.07 to 2.3 % (equivalent to relative humidity (RH) of 3–90 %). According to Li et al. (2015), UV photon fluxes (abbr. UV hereafter) at 185 and 254 nm are estimated to be in the ranges 1.0×10^{11}–1.0×10^{14} and 4.2×10^{13}–8.5×10^{15} photons cm^{-2} s^{-1}, respectively. Four levels of OHR$_{ext}$, 0, 10, 100, and 1000 s^{-1} covering the range of most field and laboratory studies are investigated. In the explored parameter space, the same 3-character labels as in Peng et al. (2015) are used to denote typical cases (Table 1). For OFR254, we study OFR254-70 and OFR254-7, representing OFR254 experiments with high (Palm et al., 2015) and low O$_3$ (Kang et al., 2011; Liu et al., 2015), respectively. To model literature OFR studies, we adopt corresponding parameters (reactor volume, H$_2$O, residence time, etc.), and estimate some (e.g., UV) as needed. In particular, for some field studies, where long time-series of experimental data [42 d in BEACHON-RoMBAS (Palm et al., 2015), 42 d in SOAS (Hu et al., 2015), and 15 d in CalNex-LA (Ortega et al., 2015)] were recorded, we model all moments when data are available and present outputs in the form of histograms.

3 Results and discussions

In the following sections we explore the relative importance of those five non-OH pathways (photons at 185 and 254 nm, O(^{1}D), O(^{3}P), and O$_3$) vs. the OH reaction for species of atmospheric interest, including a variety of typical biogenic and anthropogenic VOCs and a few important inorganic species (e.g., SO$_2$ and NO$_2$). Because of the huge complexity of VOC oxidation mechanisms, only consumption/oxidation of specific VOCs is investigated. In such an investigation, a large amount of kinetic data is

required. We collected the required data (Tables S1–S3 in the Supplement) according to the principles in Sect. S1 in the Supplement. Photolysis of SOA, a pathway ignored in previous OFR studies, is also investigated.

3.1 Fractional loss of VOCs to non-OH reactants

As shown in Peng et al. (2015), OH_{exp} in OFRs depends on various physical conditions, e.g., H_2O and OHR_{ext}. However, the non-OH reactants are much less dependent on these parameters. H_2O and external OH reactants only contribute less than 1 % to absorption at 185 and 254 nm. Therefore, they have almost no impact on effective UV. O_3 can absorb a fraction of the 254 nm radiation, but the optical depth due to 70 ppm O_3 in the reactor is ~ 0.11, and thus the attenuation of 254 nm photons by O_3 absorption is a minor effect. The dominant fates of $O(^1D)$ and $O(^3P)$ are the quenching by air and the recombination with O_2, respectively, with which no reactions involving H_2O or external OH reactants can compete. Thus the concentrations of $O(^1D)$ and $O(^3P)$ in the reactor depend on UV intensity and H_2O, but not on OHR_{ext}. Since OH can be strongly modulated by OHR_{ext}, changing physical conditions may result in very different relative importance of OH to other reactive species. To fully evaluate this issue, it is necessary to explore a very wide range of conditions as in Peng et al. (2015).

3.1.1 Common features of all the non-OH reactants

Figures 1–5 show the relative consumption of several species vs. ratio of exposures to individual non-OH species (X) to OH exposure (X_{exp}/OH_{exp}) for 185 and 254 nm photons, $O(^1D)$, $O(^3P)$, and O_3, respectively. Figures S1–S5 present the same information in an alternative format that may be useful to evaluate the fate of species not included in our study. They show ratios of rate constants of species with OH to those with non-OH species (X), mathematically equivalent to the X_{exp}/OH_{exp} where corresponding $X/(OH + X)$ is 50 %. $X/(OH + X)$ denotes the fractional importance of X in the sum of the contribution of OH and X to VOC. If a VOC has a higher ratio of rate

constant with OH to that with a non-OH reactant (X) than with another reactant (Y), the relative contribution of X, $X/(OH + X)$, should be smaller than that of Y. In these figures, we also show the X_{exp}/OH_{exp} range for OFR254-70, OFR254-7, and OFR185, under different conditions, including key laboratory and field studies, and identify the X_{exp}/OH_{exp} ranges where non-OH contribution to species fate is significant. A dissociation quantum yield of unity is assumed for the photolysis reactions, which results in upper limits for the relative importance of those pathways.

In these figures, the relationships of all non-OH reactive species to OH are similar for certain common conditions. Under "pathological conditions" of high/very high OHR_{ext} ($\geq 100\,s^{-1}$) and/or low RH (3 %), non-OH reactions can be significant depending on the species. Conversely, under low OHR_{ext} and high RH, reaction with OH is dominant (Figs. S1–S5). High H_2O and zero/low OHR_{ext} lead to strong OH production and no/weak OH suppression, respectively. Thus, OH is more abundant and dominates species consumption under those conditions. In the case of low H_2O and high OHR_{ext}, OH is generally lower because of less production and more suppression. These conditions increase the relative contribution of non-OH species. UV light intensity is generally less influential on non-OH VOC fate than H_2O and OHR_{ext}, although OH production is nearly proportional to UV (Peng et al., 2015), because the non-OH reactive species also scale (nearly) proportional to UV. As a result, UV only has minor effects on exposure ratios between OH and the non-OH reactants. In addition to the common features above, individual non-OH reactants have their own features as well as a few exceptions to the abovementioned general observations, which we will detail below.

3.1.2   Reactions with OH vs. photolysis at 185 nm

At a low H_2O volume mixing ratio of 0.0007 (RH = 3 % at 22 °C) and $OHR_{ext} \geq 100\,s^{-1}$, photolysis at 185 nm of several aromatic compounds, such as toluene, benzene, and p-xylene, are estimated to be significant and even dominant vs. the OH reactions (Fig. 1). This results from their aromatic ring, which is not only highly efficient as a chromophore, but also relatively resistant to OH attack.

It is not common to perform field studies for SOA at RH as low as 3 % or $OHR_{ext} \geq$ 100 s^{-1} (Table 1). According to $F185_{exp}/OH_{exp}$ calculated from the field studies where OFR185 was deployed, i.e., BEACHON-RoMBAS (Palm et al., 2015), SOAS (Hu et al., 2015), and CalNex-LA (Ortega et al., 2015) (ambient OH reactivity estimated to be $\sim$ 15–25 s^{-1}), by our model, none of these field studies fell into the conditions where the fractional importance of photolysis at 185 nm was significant for aromatic species. However, in some source studies using OFRs, e.g. when sampling biomass burning smoke (FLAME-3; Ortega et al., 2013) or air in a traffic tunnel (Tkacik et al., 2014), OHR_{ext} can be very high reaching values of several 100 s^{-1} (Table S4). Especially on the smoke study, photolysis of aromatics may have played a role. However, it has long been known that excited aromatic molecules may undergo various deactivation pathways (e.g., vibronic coupling, intersystem crossing, and collisional quenching) without molecular fragmentation (Beddard et al., 1974; Nakashima, 1982; Nakashima and Yoshihara, 1983; Fang and Phillips, 2002), preventing unity quantum yields. Therefore, the photolysis of aromatics at 185 nm in the abovementioned source studies may not be as significant as estimated in Fig. 1.

Under pathological conditions (low RH and/or high OHR_{ext}), some organic nitrates (e.g., peroxyacetyl nitrate and 2-propyl nitrate in Fig. 1) have a contribution from photolysis at 185 nm to their fate that is comparable to or even larger than that of reaction with OH. Nevertheless, this does not mean that we need to make extra efforts to avoid the photolysis of organic nitrates at 185 nm. Although they have cross-sections at 185 nm $\sim$ 10–100 times smaller than those of aromatics, these organic nitrates react remarkably slowly with OH ($\sim$ 2 order of magnitude slower than reactions of aromatics with OH), so photolysis appears substantial with respect to reaction with OH. However, absolute photolyzed amounts of these nitrates are not substantial. For example, only $\sim$ 10 % of peroxyacyl nitrate is photolyzed by 185 nm photons at the highest OFR185 lamp setting. Even if photolysis of nitrates by low-pressure Hg lamp emissions proceeds to a significant extent, it may still not be a problem, as it generally leads to the same products as their ambient photolysis (Renlund and Trott, 1984; Roberts and Fa-

Title Page

Abstract | Introduction

Conclusions | References

Tables | Figures

|◄ | ►|

◄ | ►

Back | Close

Full Screen / Esc

Printer-friendly Version

Interactive Discussion

jer, 1989). Nitrate photolysis is actually much more important in the atmosphere than in OFRs for the same photochemical age (Fig. 6).

SO$_2$ has been used in some studies to calibrate OH$_{exp}$ (Lambe et al., 2015; Li et al., 2015). It does undergo significant photolysis at 185 nm under pathological conditions.

5 However, this photolysis does not lead to an overestimation of OH$_{exp}$, since one of the products of SO$_2$ photolysis at 185 nm, SO, converts back to SO$_2$ very rapidly through its reaction with O$_2$.

3.1.3 Reactions with OH vs. photolysis at 254 nm

The photon flux in the reactor at 254 nm is 80–250 times larger than at 185 nm (Li et al.,
10 2015). Although absorption cross sections of all molecules investigated in this study are much lower at 254 than 185 nm, the higher photon flux approximately compensates for this effect, so that in OFR185 photolysis at 254 nm is of similar relative importance as photolysis at 185 nm, with potentially important effects at low H$_2$O and/or high OHR$_{ext}$ (Figs. 2 and S2). As for 185, 254 nm photolysis is a concern mainly for aromatic com-
15 pounds, because of the high light absorptivity and low OH reactivity of aromatic rings as previously discussed. Again, note that this concern may be less serious than shown in Fig. 2 because of possible lower quantum yields. Photolysis of organic nitrates at 254 nm also appears to be important relative to reactions with OH, and is still not a concern for the same reasons as photolysis at 185 nm. SO$_2$ can absorb efficiently
20 at 254 nm, but it is still not a problem for SO$_2$-based OH$_{exp}$ calibration, since photons at 254 nm are not sufficiently energetic to dissociate SO$_2$ molecules.

High UV generally appears to be more pathological than low UV in OFR254 (Fig. S2). This is in contrast to the trend of OFR185. In OFR254, O$_3$ is the only primary OH source, and a substantial fraction of O$_3$ can be photolyzed at the highest lamp set-
25 tings, leading to a substantial reduction of OH production (compared with proportional scaling with UV). OFR254-70 appears to be less prone to pathological conditions than OFR254-7, since higher O$_3$ favors HO$_2$-to-OH recycling, making OH more resilient to suppression (Peng et al., 2015).

Under highly pathological conditions, some saturated ketones (e.g., methyl ethyl ketone and hydroxyacetone) have significant photolysis at 254 nm relative to reactions with OH. Significant relative contribution of photolysis also results from remarkably slow reactions of saturated ketones with OH. Although secondary species without C=C double bond, e.g., saturated carbonyls, hydroperoxides, and nitrates, can be photolyzed in OFRs at low RH and/or high OHR_{ext}, their photolysis only proceeds to a $\sim$ 10–1000 times smaller extent than ambient photolysis at the same photochemical age (Fig. 6).

As discussed for photolysis at 185 nm, in all ambient OFR field studies (BEACHON-RoMBAS, SOAS, and CalNex-LA), reactions with OH dominate over photolysis at 254 nm (Fig. 2). The fractional consumption of several anthropogenic aromatic VOCs, such as benzene and naphthalene, in the urban CalNex-LA campaign by 254 nm photolysis is estimated as a few percent under most conditions and at most $\sim$ 15 %. At the BEACHON-RoMBAS and SOAS forested sites, photolysis at 254 nm should be a negligible contributor to the fate of biogenic VOCs such as isoprene and monoterpenes.

Some laboratory and source studies may have had an appreciable contribution to aromatic species fate from 254 nm at low RH and/or high OHR_{ext}. $F254_{exp}/OH_{exp}$ in the biomass smoke and urban tunnel source studies (source OHR_{ext} up to $\sim$ 300 s^{-1}; Ortega et al., 2013; Tkacik et al., 2014) and the Kang et al. (2011) laboratory study (RH down to $\sim$ 3 %) can be as high as 10^6–10^7 cm s^{-1}. In this range, photolysis of a few aromatic VOCs (e.g., benzene and naphthalene) at 254 nm could account for $\sim$ 20–80 % of their destruction.

Note that in field and source studies, where the composition of VOCs is highly complex, the presence of common aromatic species such as benzene and naphthalene is likely. In contrast, in laboratory studies, the identity of the VOC is usually well controlled. Only the precursor and its oxidation intermediates, usually oxygenated species (e.g., ketones, aldehydes, and alcohols), need to be considered. Therefore, one may conduct laboratory experiments with OFRs under conditions that would be pathological for some field or source studies, if photolysis of the specific studied species and corresponding intermediates at 254 nm is not significant in its destruction. For exam-

ple this is the case for the experiments with α-pinene in Kang et al. (2011), and those with isoprene in Lambe et al. (2011b). In all these experiments, the fractional photolytic consumption of the precursors by 254 nm photons is less than 1 %. The fractional consumption of oxygenated intermediates is also just a few percent, even if we assume that all intermediates have as high a relative photolytic impact as methyl ethyl ketone. Lambe et al. injected isoprene at OHR_{ext} as high as 792 s^{-1} into their OFR (Table S4) which is expected to reduce the OH concentration according to the modeling results of Peng et al. (2015), but the relative impact of isoprene photolysis at 254 nm is still negligible thanks to the very rapid reaction of isoprene with OH.

However, Klems et al. (2015)'s experiment with dodecanoic acid may have had a significant fractional impact from photolysis at 254 nm, although photolysis of the precursor is negligible compared to its reaction with OH. The OFR used by Klems et al. (2015) has a different design from the PAM, which is regarded as the base design in this study. Their reactor employs a light source stronger than the PAM's highest lamp setting, with UV estimated to be $\sim 3 \times 10^{16}$ photons cm^{-2} s^{-1} based on the lamp power and the reactor geometry. Such high UV may result in significant photolysis of carbonyl intermediates, which are very likely formed in the oxidation of long-chain alkane-like dodecanoic acid. Photolysis of carbonyls often lead to carbon-chain cleavage via Norrish reaction (Laue and Plagens, 2005), which may account for some of large amounts of fragmentation products observed in the Klems et al. (2015) experiments.

3.1.4 Reactions with OH vs. reactions with O(^{1}D) and O(^{3}P)

The results for these two radicals are shown in Figs. 3 and 4. The potential impact of O(^{1}D) is smaller than for 185 and 254 nm photons, due to the low concentration of O(^{1}D) in the reactor. Only for methane may reaction with O(^{1}D) be significant, because the reaction of methane with O(^{1}D) is close to the collision rate, while CH$_4$ is the most resistant VOC to H-abstraction by OH. This could be important if CH$_4$ was used for OH_{exp} calibration under pathological reactor conditions, or if the fate of CH$_4$ is important

to the experiment for other reasons. Other VOCs react more slowly with $O(^1D)$ and much faster with OH. As a result, reactions of VOCs (other than CH_4) with $O(^1D)$ in all laboratory, field, and source studies previously discussed are almost always negligible. We also note that the ratio of $O(^1D)_{exp}/OH_{exp}$ in the OFR is actually much lower than in the troposphere (Monks, 2005), except under some pathological conditions. It is believed that the contribution of O atoms to VOC destruction in the atmosphere should be negligible (Calvert et al., 2002), and their relative importance is even lower under most OFR conditions.

Reactions with $O(^3P)$ are small or negligible contributors to VOC consumption except under extreme pathological conditions. Unless at low H_2O and very high external OH reactivity ($1000\,s^{-1}$), VOC consumption by $O(^3P)$ cannot be larger than 10% of that by OH (Figs. 4 and S4). This results from both very low concentrations of $O(^3P)$ and relatively low reactivity compared to that of OH. Among the species that we examine, biogenic VOC consumption may have some contribution from $O(^3P)$ under the above mentioned pathological condition, due to the high reactivity of double bonds in these species with $O(^3P)$. For example the isoprene experiments in Lambe et al. (2011b) may have had a $\sim 5\%$ contribution from $O(^3P)$. Similarly to $O(^1D)$, $O(^3P)_{exp}/OH_{exp}$ in the troposphere (Calvert et al., 2002) is higher than in the OFR except for pathological conditions. Thus the relative importance of O atoms to OFR chemistry is typically lower than in the troposphere.

3.1.5 Reactions with OH vs. reactions with O_3

Reaction with O_3 is a major, even dominant pathway of the consumption of many biogenic VOCs in the troposphere. However, it is of interest to quantify the relative importance of OH vs. O_3 across OFR experiments (Figs. 5 and S5). This allows comparison with the relative importance in the troposphere, as well as potentially designing experiments where the influence of O_3 is minimized.

A large amount of O_3 is injected into OFR254, and O_3 concentration in that type of reactor does not change much with UV flux (negligibly under most conditions and up to a factor of 2 at high H_2O and UV, Peng et al., 2015). Since OH_{exp} is proportional to UV flux, as UV decreases, OH_{exp} is lowered and the fractional species destruction by O_3 increases. In OFR185, O_3 production is almost linearly dependent on UV, while a significant portion of OH production has a quadratic relationship with UV. Thus OH increases faster with increasing UV than O_3. Therefore, lower UV in OFR185 also leads to a higher relative importance of O_3 for VOC consumption.

The distribution of O_{3exp}/OH_{exp} expected for the troposphere was obtained from the GISS ModelE2 climate model (Schmidt et al., 2014) and is estimated as the ratio of the simulated daily mean concentration of O_3 and OH on a horizontal grid of 2° in latitude and 2.5° in longitude for the year 2000. Interestingly, the simulated relative importance of O_3 to OH in the troposphere is higher than when OFRs are operated under normal conditions, and similar to OFRs when they are operated under pathological conditions (Figs. 5 and S5). In those cases, a number of biogenic VOCs can be significantly consumed by O_3. In particular, some monoterpenes (e.g., α-terpinene) and sesquiterpenes (e.g., β-caryophyllene) have a fractional reaction with O_3 close to 100 % in the troposphere. In contrast to biogenics, reactions with O_3 do not play any role in the consumption of most anthropogenic VOCs, e.g., benzene, toluene, and alkanes. Besides, ozonolysis of saturated oxidation intermediates (e.g. carbonyls and alcohols) is minor or negligible in both OFRs and the atmosphere, since they react with OH at $\sim 10^{-13}$–10^{-11} cm^3 molecule^{-1} s^{-1} while their ozonolysis rate constants are $< 10^{-20}$ cm^3 molecule^{-1} s^{-1} (Atkinson and Arey, 2003). It has to be noted though that the values used from the model are daily means, which underestimates the amount of OH in the atmosphere during daytime by roughly a factor of 2.

An experimenter may be interested in obtaining an O_{3exp}/OH_{exp} in an OFR close to the ambient values, which requires low RH and high OHR_{ext} conditions. On the other hand, one may want to study OH-dominated chemistry and thus wants to avoid significant ozonolysis of VOCs. In that case the OFRs should be operated under opposite

conditions, i.e., high H_2O, high UV, and low OHR_{ext}. This strategy enhancing OH_{exp} is effective for most VOCs, except those with the highest k_{O_3}/k_{OH} ratios, e.g., α-terpinene and β-caryophyllene. To further decrease the importance of reactions of VOC with O_3, it is necessary to lower the O_3 concentration. For OFR254, one can inject less O_3 into the reactor and increase the UV lamp setting. The comparison between OFR254-70 and OFR254-7 in Fig. 5 demonstrates this approach. For OFR185, we propose another strategy, i.e., lowering O_2 concentration in the reactor. This decreases O_3 production but affects OH production to a much lesser extent, thanks to the major OH production by H_2O photolysis. We simulate the OFR185 cases with 2‰ O_2 and observe that VOC ozonolysis can be excluded at high H_2O and high UV (Fig. S5).

Among the literature OFR studies, the field studies employing OFRs in urban and forested areas all operated under O_{3exp}/OH_{exp} values 100 times lower than in the atmosphere. In these field studies reaction of almost all VOCs with O_3 can be neglected, except for the most reactive biogenics with O_3, e.g., α-terpinene and β-caryophyllene. The source study in an urban tunnel of Tkacik et al. (2014) operated under similar conditions. Some laboratory studies using OFR254 (Kang et al., 2011; Lambe et al., 2011b) as well as the biomass smoke source study (Ortega et al., 2013) operated at O_{3exp}/OH_{exp} close to tropospheric values, because the injected O_3 plays a key role for OFR254 studies and the biomass smoke experiments were conducted at high OHR_{ext}. Nevertheless, only α-pinene and β-pinene, both biogenics, are significantly consumed by O_3. Another OFR254 study, Klems et al. (2015), had O_{3exp}/OH_{exp} significant lower than tropospheric values, since the initial O_3 in their experiment was only 2 ppm, and the UV light in their experiment was stronger than our lamps' highest setting and further reduced effective O_3.

3.1.6   Reactions with $^1O_2$ and HO_2

Singlet oxygen, $^1O_2$, can be produced in various ways in OFRs (Calvert et al., 2002; Ono et al., 2014) and react with alkenes at appreciable rate constants ($\sim 10^{-17}$–

10^{-14} cm^3 molecule^{-1} s^{-1}; Huie and Herron, 1973; Eisenberg et al., 1986). We estimate $^1O_2$ concentration by the expression proposed by Ono et al. (2014). Only at the lowest RH, the highest lamp setting, and the highest OHR$_{ext}$ in this study (Table 1), may the most reactive alkene (endo-cyclic conjugated dienes, e.g., cyclopentadiene, α-terpinene, and α-phellandrene) have > 10 % contribution from $^1O_2$ to their fate. For all other species and under all other conditions, reactions of VOCs with $^1O_2$ are negligible. Thus, this reactant is not discussed further in the present work.

HO$_2$ is a major radical in the OFR chemistry. However, it is much less reactive than OH toward VOCs. Typically, the rate constants of reactions of HO$_2$ with alkenes are smaller than 10^{-20} cm^3 molecule^{-1} s^{-1} at room temperature, and those with saturated VOCs are even smaller (Tsang, 1991; Baulch et al., 1992, 2005). Therefore, all reactions of HO$_2$ with VOCs can be simply neglected in this study.

3.1.7 Overall contribution of non-OH reactants to gas-phase chemistry

In this section we summarize the combined effect of all non-OH reactants to VOC consumption. However, we can no longer use X$_{exp}$/OH$_{exp}$ to express total non-OH VOC consumption as for individual reactants. Total non-OH VOC consumption is thus discussed case by case.

In the explored range of conditions (i.e., RH, UV, OHR$_{ext}$, and initial O$_3$ for OFR254), there are obviously conditions where all non-OH fates of VOCs are negligible. Most simply, the highest RH and UV in this study and a very small non-zero OHR$_{ext}$ result in a VOC consumption nearly 100 % by OH, regardless of the VOC type (Table S5). Lowering UV can make non-OH contribution even smaller for OFR185, but not for OFR254. This difference occurs because OH production is reduced while O$_3$ roughly remains at the same level in OFR254, leading to enhanced relative contribution from O$_3$ to the fate of biogenics. At the lowest non-zero UV in Li et al. (2015)'s PAM reactor (7.9×10^{11} photons cm^{-2} s^{-1} at 185 nm; 2.0×10^{14} photons cm^{-2} s^{-1} at 254 nm), the fractional destructions of α-pinene (representative of biogenic VOCs) by O$_3$ are 21 and

Non-OH chemistry in oxidation flow reactors

Z. Peng et al.

4.2 % in OFR254-70 and OFR254-7, respectively. Other OFR designs may reach lower UV, e.g., the "low UV" case defined in this study (1.0×10^{11} photons cm^{-2} s^{-1} at 185 nm; 4.2×10^{13} photons cm^{-2} s^{-1} at 254 nm). At these UV levels, the fate of α-pinene by O_3 further increases to 44 and 13 % in OFR254-70 and OFR254-7, respectively.

On the other hand, non-OH reactants can dominate VOC fate under opposite conditions that lead to low OH production and strong OH suppression. At the lowest RH and UV and the highest OHR$_{ext}$ in this study, > 95 % of α-pinene and ~ 80 % of toluene are consumed by non-OH reactants in OFR185. In OFR254, almost all α-pinene has non-OH fate while non-OH fate of toluene is still minor or negligible. If OFRs are operated at the low UV setting from Li et al. (2015)'s PAM, ~ 8 times higher the lowest UV in this study, the situation hardly changes, as a very large OH suppression persists. Nevertheless, if UV is increased to the highest level, non-OH fate of α-pinene is lowered to ~ 60–70 % and that of toluene in OFR185 decreases to 24 %. When RH is at the highest level, non-OH fate is systematically lower than at low RH in all types of OFRs. In particular, Case HHV has non-OH fates of α-pinene only up to ~ 10 % and negligible non-OH fates of toluene, despite very high OHR$_{ext}$.

We also summarize VOC fate for key laboratory, source, and field studies examined in the present work in Fig. 7. For each case, the fate of one or a few typical VOCs is investigated. In laboratory studies, Kang et al. (2011) performed experiments with a mixture of α-pinene, m-xylene, and p-xylene, and one of Lambe et al. (2011b)'s experiments used biogenics (α-pinene and isoprene, respectively) as precursors. In both cases, O_3 plays a role in the fate of biogenics when RH is low (Kang et al.), or OHR$_{ext}$ is high and UV is low (Lambe et al.), as shown in Fig. 7. The fate of isoprene by O_3 is less significant despite the very high OHR$_{ext}$, because isoprene, compared to α-pinene, is more reactive with OH and less reactive with O_3. Besides, O(^{3}P) contributes a few percent to the fate of both biogenics. In the literature experiments performed at a higher RH (Kang et al.) or a higher UV (Lambe et al.), non-OH fate of both VOCs significantly decreases because of increases in OH$_{exp}$. However, the contribution of O(^{3}P) to isoprene fate almost remains the same, since both OH and O(^{3}P) increase with UV.

About 20 % of p-xylene in Kang et al. (2011)'s mixture experiment at very low RH may be destroyed by 254 nm photons. Other laboratory study cases with aromatics have lower non-OH fates because of higher RH. n-decane in one of Lambe et al. (2011b)'s experiments and dodecanoic acid in Klems et al. (2015)'s study are consumed ~ 100 % by OH, as these alkane(-like) species neither react rapidly with O_3, nor absorb UV efficiently. However, as previously discussed, some carbonyl compounds may be formed and significantly photolyzed at 254 nm in Klems et al. (2015)'s experiments, although the huge complexity of intermediates and limited knowledge of reaction mechanisms prevents a quantitative assessment of the fate of carbonyl intermediates by photons at 254 nm.

Source and field studies usually have highly complex precursors. For the urban tunnel study (Tkacik et al., 2014) and the CalNex-LA study in the Los Angeles basin (Ortega et al., 2015), we choose toluene as a representative of aromatic species, as these are major anthropogenic VOCs and SOA precursors in urban environment (Dzepina et al., 2009; Borbon et al., 2013; Hayes et al., 2015; Jathar et al., 2015). Although alkanes are also major anthropogenic VOCs, their non-OH fate is not quantitatively assessed for the same reason as discussed for dodecanoic acid in Klems et al. (2015)'s experiment. For the smoke aging study, FLAME-3 (Ortega et al., 2013), we select benzene and α-pinene, which are important VOCs in biomass burning emissions (Warneke et al., 2011). For the BEACHON-RoMBAS and SOAS studies at forested sites, α-pinene and isoprene are chosen, respectively, as they are major emitted biogenic VOCs at those corresponding sites. Both the urban tunnel and FLAME-3 studies have aromatic precursors significantly photolyzed at 185 and 254 nm under the conditions of high source concentrations (Fig. 7). The toluene fate by UV in the tunnel study is less substantial than that of benzene in FLAME-3, since NO_x, the largest fraction of external OH reactant in the tunnel study, is converted into HNO_3 very rapidly (Li et al., 2015) and does not further suppress OH. In the cases of lower OHR_{ext} (e.g., the tunnel experiments with low source concentration and CalNex), toluene is dominantly consumed by OH. It also holds for biogenic VOCs that non-OH fate decreases with decreasing

OHR$_{ext}$ due to less OH suppression. The non-OH fate of α-pinene in FLAME-3, dominated by reaction with O$_3$, is larger than 20 %, while the non-OH fates of α-pinene in BEACHON-RoMBAS and of isoprene in SOAS are both negligible, since OHR$_{ext}$ in the former study is > 10 times higher than in the latter two studies.

3.2   SOA photolysis

Recently, photolysis has been found to be a potentially significant sink of some types SOA in the troposphere (Wong et al., 2015; Hodzic et al., 2015). It is necessary to also investigate SOA photolysis in OFRs, as photons used in OFRs are highly energetic and non-tropospheric. UV extinction due to aerosol optical scattering and in-particle absorption is generally negligible (Hodzic et al., 2015). For simplicity, we estimate photodegradation ratios of various possible SOA components (Fig. 8) under the assumption of unity quantum yield. Therefore, the estimates are actually the upper limits of photodegradation ratios. We use surrogate gas-phase species for the different functional groups as the cross sections of SOA-relevant species at these wavelengths are not available, as done in other studies (Hodzic et al., 2015).

Most SOA functional groups are oxygenated (e.g., peroxides, carbonyls, carboxylic acids, alcohols). The absorption cross sections of most of these functional groups are too low at 185 and 254 nm given the OFR residence time and UV light intensity, leading to a small contribution of photolysis to SOA degradation (Fig. 8). For example, glycolaldehyde has a negligible fractional contribution of photolysis except at the highest lamp setting, when only ~ 5 % of this species photolyzes at each wavelength. Species (e.g., isoprene) with conjugated double bonds as efficient chromophores will not be present in SOA because of their high reactivity with OH and O$_3$. Nitrate groups may have a ~ 30 % contribution from photolysis at the highest UV settings, and a negligible contribution at intermediate or low UV settings.

Aromatic rings are more resistant to OH attack and usually strongly absorb UV light. Under our assumptions, the photolysis of some aromatic SOA components (e.g., o-cresol at 185 nm and naphthalene at 254 nm) is already important at medium UV flux.

At the highest lamp setting, most aromatics in SOA would be destroyed if the quantum yields are indeed near unity. However, as previously discussed, photolysis quantum yields of aromatics may be significantly lower than 1. This is more probable in the condensed phase (Damschen et al., 1978; Baker et al., 2015) than in the gas phase, as quenching processes in the condensed-phase matrix are usually much more efficient than through gas-phase molecular collisions. It has recently been reported that photolysis quantum yields of aromatics in SOA were low under UVB irradiation (Romonosky et al., 2015). Although the range and relevance of the species investigated in that study are limited, it is reasonable to assume low quantum yield for aromatic photolysis in SOA at 185 and 254 nm. On the other hand, direct measurements are desirable for this issue and caution should still be exercised for OFR experiments at high UV for aromatic SOA systems.

For most SOA components, photolysis is unimportant in OFRs in terms of absolute photolyzed amount. This is also true compared to ambient SOA photolysis. OH_{exp} in OFRs is normally on the order of 10^{11}–10^{13} molecules cm^{-3} s, equivalent to photochemical ages of a day to several months. Case HHH (Table 1) is one of the cases just outside the pathological region, i.e., with the highest photon-to-OH ratio and without problems of non-tropospheric chemistry. OH_{exp} is $\sim 2 \times 10^{13}$ molecules cm^{-3} s in this case. Hodzic et al. (2015) estimated an average ambient SOA photolysis lifetime of 3.5 days. Therefore, on average, ambient SOA may undergo ~ 40 generations of photolysis (1 generation of photolysis means that the species concentration decreases by a factor of e due to photolysis) in the troposphere before it is as OH-aged in ambient air as in Case HHH in OFRs. Some components in SOA (e.g., glyoxal and 2-methylpropanal) may proceed with more than 500 generations of ambient photolysis before they reach an ambient OH exposure comparable to in an OFR. In contrast, only 5 generations of photolysis at most have occurred on SOA in Case HHH in OFRs (Table S6). Except for species that do not photolyze in the troposphere, the photolysis of all SOA components proceeds to an extent of at least one order of magnitude smaller than that in the troposphere (Table S6). Although the photolysis products may be dif-

ferent at the different wavelengths, this result indicates that the relative importance of SOA photolysis is much lower in OFRs compared to the troposphere. Nevertheless, aromatic photolysis in SOA may lead to different chemistry in OFRs from that in the troposphere, if this type of photolysis really occurs to a significant extent.

3.3 Guidelines for OFR experimental design and operation

It is necessary to avoid significant non-tropospheric chemistry in OFRs in order to more faithfully simulate tropospheric aging. Only photolysis at 185 and 254 nm are important non-tropospheric pathways in OFRs and reactions with O atoms are generally unimportant. Ozonolysis is also a major VOC sink in the troposphere, and the desirability of including or excluding its effects depends on the goals of each experiment.

In the cases where the exclusion of VOC ozonolysis is desired, there is no dilemma for the experimental design, as the exclusion of both VOC ozonolysis and non-tropospheric VOC consumption requires similar conditions, i.e., high H_2O and low OHR_{ext}, opposite to the "pathological" conditions. As shown above, all examined field studies do not have significant non-tropospheric contribution to VOC fate, while some past laboratory and source studies do because of low RH and/or very high OHR_{ext} in those experiments. It is possible to improve the latter experiments by increasing RH and/or lowering OHR_{ext}. In detail, source humidification and dilution can be feasible measures to increase RH and decrease OHR_{ext}, respectively. For example, increasing RH from 3 to 60 % lowers the percentage of non-tropospheric consumption of p-xylene in Kang et al. (2011)'s mixture experiment from ~ 20 to 1.5 %. Also, a 5-fold source dilution in FLAME-3 reduces the non-tropospheric fate of benzene from > 60 to ~ 15 % (Table S4 and "Improved" cases in Fig. 7). Injecting less precursor is a simple way to keep a reasonably low OHR_{ext} in laboratory studies. The comparison between the cases with high and low concentrations in the urban tunnel study (Tkacik et al., 2014) is a good example (Table S4 and Fig. 7). Note that when taking the measures above to limit non-tropospheric VOC fate, one generally reduces the contribution from all non-OH reactants. Increasing RH and source dilution also significantly lower the relative

importance of ozonolysis in the fate of α-pinene in Kang et al. (2011)'s mixture experiments and the FLAME-3 study (Table S4 and Fig. 7). Although increasing UV may increase OH production, OH reactant destruction, and hence the relative contribution of OH to VOC fate in some cases, one has to be cautious when taking this measure to reduce effective OHR_{ext}, as high UV may cause non-tropospheric photolysis of aromatic SOA components.

In laboratory experiments, usually with a single VOC or a relatively simple mixture, there is much more flexibility for experimental design to include ozonolysis while excluding non-tropospheric VOC consumption, since it is sufficient to ensure the insignificance of non-tropospheric consumption of only the component(s) and possible intermediates (usually oxygenated species), rather than for a large variety of VOC precursors. For example, we may perform OFR experiments with a large amount of biogenics at low H_2O as long as the experiment is not conducted under extremely pathological conditions. In this case, a tropospheric O_{3exp}/OH_{exp} can be perfectly obtained without major side effects, because the fractional contribution of photolysis of biogenics and possible intermediates (e.g., ketones) at 185 and 254 nm is still minor or negligible. On the other hand, OFR experiments with anthropogenic VOCs, such as alkanes and alkylbenzenes, can just be conducted at high RH and low OHR_{ext} to avoid the contribution of all non-OH reactants, since ozonolysis of alkanes and alkylbenzenes is negligible even at a tropospheric O_{3exp}/OH_{exp}.

A challenge of OFR operation is to explore the low OH_{exp} region without making non-OH VOC fate significant, as lowering RH and increasing OHR_{ext} not only reduce OH_{exp}, but also enhance non-OH VOC consumption. In principle, to obtain OH_{exp} as low as possible while avoiding significant non-OH VOC fate, RH should be as high as possible and UV should be as low as possible. High RH is highly effective in elevating the relative importance of VOC destruction by OH. In addition, it does not increase OH_{exp} by orders of magnitude compared to low RH cases. High UV does not necessarily avoid non-OH VOC consumption and increases OH_{exp} by orders of magnitude compared to low UV cases. For OFR185, OHR_{ext} is the only parameter that can be tuned to make a compro-

mise between low OH_{exp} and low non-OH VOC fate. In Li et al. (2015)'s PAM OFR, UV at 185 and 254 nm can be down to 7.9×10^{11} and 2.0×10^{14} photons cm^{-2} s^{-1}. According to our model, OHR_{ext} may be as high as ~ 100 s^{-1} to ensure that the non-OH fates of both α-pinene (biogenic) and toluene (anthropogenic aromatic) is less than 10 %. In this case, OH_{exp} as low as $\sim 3 \times 10^{10}$ molecules cm^{-3} s^{-1} can be obtained. If UV intensities at 185 nm down to 10^{11} photons cm^{-2} s^{-1} are used, an OHR_{ext} of ~ 80 s^{-1} can still keep non-OH fates of α-pinene and toluene below 10 %, and results in an OH_{exp} of $\sim 4 \times 10^9$ molecules cm^{-3} s^{-1}. In OFR254, since initial O_3 and OHR_{ext} are both tunable parameters and have antagonistic effects in avoiding non-OH VOC fate, there is a range for both parameters as long as O_3 is sufficiently low to keep VOC fate dominantly by OH. In Li et al. (2015)'s OFR, initial O_3 can be as high as ~ 800 ppb to avoid α-pinene fate by ozonolysis larger than 10 %. Accordingly, OHR_{ext} is allowed to be up to ~ 10 s^{-1} to obtain the fates of both α-pinene and toluene by OH larger than 90 %. As a result, OH_{exp} can be as low as $\sim 1.2 \times 10^{11}$ molecules cm^{-3} s^{-1}. If the lowest UV 254 nm in this study (4.2×10^{13} photons cm^{-2} s^{-1}) is reached, OH_{exp} can be lowered to $\sim 2.5 \times 10^{10}$ molecules cm^{-3} s^{-1} without causing significant destruction of α-pinene and toluene significantly by non-OH reactants. A typical condition to obtain this OH_{exp} is ~ 100 ppb O_3 and ~ 1.2 s^{-1} OHR_{ext}.

4   Conclusions

We used a kinetic model to investigate non-OH contribution (from 185 and 254 nm photons, $O(^1D)$, $O(^3P)$, and O_3) to VOC destruction, as well as to SOA photolysis at 185 and 254 nm in OFRs. We assessed the relative significance of the VOC consumption by non-OH reactants to that by OH in OFRs and the troposphere. The only non-tropospheric reactions that can play a role under OFR conditions are photolysis at 185 and 254 nm. Their relative importance is largest under "pathological" OFR conditions

Non-OH chemistry in oxidation flow reactors

Z. Peng et al.

Title Page

Abstract	Introduction
Conclusions	References
Tables	Figures

|◄ | ►|

◄ | ►

Back | Close

Full Screen / Esc

Printer-friendly Version

Interactive Discussion

where OH is low due to low RH and/or high OHR_{ext}. Reactions of O atoms are not competitive and actually of lower relative importance (vs. OH) in OFRs than in the troposphere. VOC ozonolysis is much less important than in the troposphere under typical OFR conditions and of similar importance under pathological OFR conditions. Photolysis of aromatic SOA components at 185 and 254 nm could be significant at high UV if corresponding quantum yields were high, for which direct experimental evidence is not available. Although the reaction fates may be different, photolysis rates for a given OH_{exp} are actually at least an order-of-magnitude lower in the OFRs compared to the troposphere.

We examined some past field, laboratory, and source studies using OFRs. In the field studies of aged urban and forest ambient air, non-OH VOC fate was not important because of relatively high RH and moderate OHR_{ext}. However, some laboratory and source studies were conducted at low RH and/or high OHR_{ext}, and have significant non-tropospheric VOC consumption. Humidification and/or dilution are recommended in these cases to reduce the importance of non-tropospheric reactants. We proposed different approaches to avoid non-OH VOC consumption, as well as strategies to employ insignificant non-tropospheric photolysis and significant tropospheric ozonolysis simultaneously in laboratory experiments. Our work has implications for the interpretation of past OFR studies, and should be useful for designing and conducting future OFR experiments for atmospheric research, as well as in related applied fields.

The Supplement related to this article is available online at doi:10.5194/acpd-15-23543-2015-supplement.

References

Ammann, M., Cox, R. A., Crowley, J. N., Jenkin, M. E., Mellouki, A., Rossi, M. J., Troe, J., Wallington, T. J., Cox, B., Atkinson, R., Baulch, D. L., and Kerr, J. A.: IUPAC Task Group on Atmospheric Chemical Kinetic Data Evaluation, available at: http://iupac.pole-ether.fr (last access: July 2015), 2015.

Atkinson, R. and Arey, J.: Atmospheric degradation of volatile organic compounds, Chem. Rev., 103, 4605–4638, doi:10.1021/cr0206420, 2003.

Bahreini, R., Middlebrook, A. M., Brock, C. A., de Gouw, J. A., McKeen, S. A., Williams, L. R., Daumit, K. E., Lambe, A. T., Massoli, P., Canagaratna, M. R., Ahmadov, R., Carrasquillo, A. J., Cross, E. S., Ervens, B., Holloway, J. S., Hunter, J. F., Onasch, T. B., Pollack, I. B., Roberts, J. M., Ryerson, T. B., Warneke, C., Davidovits, P., Worsnop, D. R., and Kroll, J. H.: Mass spectral analysis of organic aerosol formed downwind of the Deepwater Horizon oil spill: field studies and laboratory confirmations, Environ. Sci. Technol., 46, 8025–8034, doi:10.1021/es301691k, 2012.

Baker, L. A., Horbury, M. D., Greenough, S. E., Coulter, P. M., Karsili, T. N. V., Roberts, G. M., Orr-Ewing, A. J., Ashfold, M. N. R., and Stavros, V. G.: Probing the ultrafast energy dissipation mechanism of the sunscreen oxybenzone after UVA irradiation, J. Phys. Chem. Lett., 6, 1363–1368, doi:10.1021/acs.jpclett.5b00417, 2015.

Baulch, D. L., Cobos, C. J., Cox, R. A., Esser, C., Frank, P., Just, T., Kerr, J. A., Pilling, M. J., Troe, J., Walker, R. W., and Warnatz, J.: Evaluated kinetic data for combustion modelling, J. Phys. Chem. Ref. Data, 21, 411, doi:10.1063/1.555908, 1992.

Baulch, D. L., Bowman, C. T., Cobos, C. J., Cox, R. A., Just, T., Kerr, J. A., Pilling, M. J., Stocker, D., Troe, J., Tsang, W., Walker, R. W., and Warnatz, J.: Evaluated kinetic data for combustion modeling: Supplement II, J. Phys. Chem. Ref. Data, 34, 757–1397, doi:10.1063/1.1748524, 2005.

Title Page

Abstract | Introduction

Conclusions | References

Tables | Figures

|◄ | ►|

◄ | ►

Back | Close

Full Screen / Esc

Printer-friendly Version

Interactive Discussion

Beddard, G. S., Fleming, G. R., Gijzeman, O. L. J., and Porter, G.: Vibrational energy dependence of radiationless conversion in aromatic vapours, P. R. Soc. A, 340, 519–533, doi:10.1098/rspa.1974.0168, 1974.

Borbon, A., Gilman, J. B., Kuster, W. C., Grand, N., Chevaillier, S., Colomb, A., Dolgorouky, C., Gros, V., Lopez, M., Sarda-Esteve, R., Holloway, J., Stutz, J., Petetin, H., McKeen, S., Beekmann, M., Warneke, C., Parrish, D. D., and De Gouw, J. A.: Emission ratios of anthropogenic volatile organic compounds in northern mid-latitude megacities: Observations versus emission inventories in Los Angeles and Paris, J. Geophys. Res. Atmos., 118, 2041–2057, doi:10.1002/jgrd.50059, 2013.

Calvert, J. G., Atkinson, R., Becker, K. H., Kamens, R. M., Seinfeld, J. H., Wallington, T. H., and Yarwood, G.: The Mechanisms of Atmospheric Oxidation of the Aromatic Hydrocarbons, Oxford University Press, USA, available at: https://global.oup.com/academic/product/the-mechanisms-of-atmospheric-oxidation-of-the-aromatic-hydrocarbons-9780195146288 (last access: July 2015), 2002.

Carlton, A. G., Wiedinmyer, C., and Kroll, J. H.: A review of Secondary Organic Aerosol (SOA) formation from isoprene, Atmos. Chem. Phys., 9, 4987–5005, doi:10.5194/acp-9-4987-2009, 2009.

Carter, W. P. L., Cocker, D. R., Fitz, D. R., Malkina, I. L., Bumiller, K., Sauer, C. G., Pisano, J. T., Bufalino, C., and Song, C.: A new environmental chamber for evaluation of gas-phase chemical mechanisms and secondary aerosol formation, Atmos. Environ., 39, 7768–7788, doi:10.1016/j.atmosenv.2005.08.040, 2005.

Cocker, D. R., Flagan, R. C., and Seinfeld, J. H.: State-of-the-art chamber facility for studying atmospheric aerosol chemistry, Environ. Sci. Technol., 35, 2594–2601, 2001.

Cubison, M. J., Ortega, A. M., Hayes, P. L., Farmer, D. K., Day, D., Lechner, M. J., Brune, W. H., Apel, E., Diskin, G. S., Fisher, J. A., Fuelberg, H. E., Hecobian, A., Knapp, D. J., Mikoviny, T., Riemer, D., Sachse, G. W., Sessions, W., Weber, R. J., Weinheimer, A. J., Wisthaler, A., and Jimenez, J. L.: Effects of aging on organic aerosol from open biomass burning smoke in aircraft and laboratory studies, Atmos. Chem. Phys., 11, 12049–12064, doi:10.5194/acp-11-12049-2011, 2011.

Damschen, D. E., Merritt, C. D., Perry, D. L., Scott, G. W., and Talley, L. D.: Intersystem crossing kinetics, J. Phys. Chem., 82, 2268–2272, doi:10.1021/j100510a002, 1978.

Dzepina, K., Volkamer, R. M., Madronich, S., Tulet, P, Ulbrich, I. M., Zhang, Q., Cappa, C. D., Ziemann, P. J., and Jimenez, J. L.: Evaluation of recently-proposed secondary organic

aerosol models for a case study in Mexico City, Atmos. Chem. Phys., 9, 5681–5709, doi:10.5194/acp-9-5681-2009, 2009.

Eisenberg, W. C., Taylor, K., and Murray, R. W.: Gas-phase kinetics of the reaction of singlet oxygen with olefins at atmospheric pressure, J. Phys. Chem., 90, 1945–1948, doi:10.1021/j100400a041, 1986.

Fang, W. H. and Phillips, D. L.: The crucial role of the S1/T2/T1 intersection in the relaxation dynamics of aromatic carbonyl compounds upon $n \rightarrow \pi^*$ excitation, ChemPhysChem, 3, 889–892, doi:10.1002/1439-7641(20021018)3:10<889::AID-CPHC889>3.0.CO;2-U, 2002.

George, I. J., Vlasenko, A., Slowik, J. G., Broekhuizen, K., and Abbatt, J. P. D.: Heterogeneous oxidation of saturated organic aerosols by hydroxyl radicals: uptake kinetics, condensed-phase products, and particle size change, Atmos. Chem. Phys., 7, 4187–4201, doi:10.5194/acp-7-4187-2007, 2007.

Hallquist, M., Wenger, J. C., Baltensperger, U., Rudich, Y., Simpson, D., Claeys, M., Dommen, J., Donahue, N. M., George, C., Goldstein, A. H., Hamilton, J. F., Herrmann, H., Hoffmann, T., Iinuma, Y., Jang, M., Jenkin, M. E., Jimenez, J. L., Kiendler-Scharr, A., Maenhaut, W., McFiggans, G., Mentel, Th. F., Monod, A., Prévôt, A. S. H., Seinfeld, J. H., Surratt, J. D., Szmigielski, R., and Wildt, J.: The formation, properties and impact of secondary organic aerosol: current and emerging issues, Atmos. Chem. Phys., 9, 5155–5236, doi:10.5194/acp-9-5155-2009, 2009.

Hayes, P. L., Carlton, A. G., Baker, K. R., Ahmadov, R., Washenfelder, R. A., Alvarez, S., Rappenglück, B., Gilman, J. B., Kuster, W. C., de Gouw, J. A., Zotter, P., Prévôt, A. S. H., Szidat, S., Kleindienst, T. E., Offenberg, J. H., Ma, P. K., and Jimenez, J. L.: Modeling the formation and aging of secondary organic aerosols in Los Angeles during CalNex 2010, Atmos. Chem. Phys., 15, 5773–5801, doi:10.5194/acp-15-5773-2015, 2015.

Hodzic, A., Madronich, S., Kasibhatla, P. S., Tyndall, G., Aumont, B., Jimenez, J. L., Lee-Taylor, J., and Orlando, J.: Organic photolysis reactions in tropospheric aerosols: effect on secondary organic aerosol formation and lifetime, Atmos. Chem. Phys., 15, 9253–9269, doi:10.5194/acp-15-9253-2015, 2015.

Hoffmann, T., Odum, J. R., Bowman, F., Collins, D., Klockow, D., Flagan, R. C., and Seinfeld., J. H.: Formation of organic aerosols from the oxidation of biogenic hydrocarbons, J. Atmos. Chem., 26, 189–222, doi:10.1023/A:1005734301837, 1997.

Hu, W. W., Campuzano-Jost, P., Palm, B. B., Day, D. A., Ortega, A. M., Hayes, P. L., Krechmer, J. E., Chen, Q., Kuwata, M., Liu, Y. J., de Sá, S. S., Martin, S. T., Hu, M., Budisulis-

Non-OH chemistry in oxidation flow reactors

Z. Peng et al.

Title Page

Abstract	Introduction
Conclusions	References
Tables	Figures

|◀ | ▶|

◀ | ▶

Back | Close

Full Screen / Esc

Printer-friendly Version

Interactive Discussion

tiorini, S. H., Riva, M., Surratt, J. D., St. Clair, J. M., Isaacman-Van Wertz, G., Yee, L. D., Goldstein, A. H., Carbone, S., Artaxo, P., de Gouw, J. A., Koss, A., Wisthaler, A., Mikoviny, T., Karl, T., Kaser, L., Jud, W., Hansel, A., Docherty, K. S., Robinson, N. H., Coe, H., Allan, J. D., Canagaratna, M. R., Paulot, F., and Jimenez, J. L.: Characterization of a real-time tracer for Isoprene Epoxydiols-derived Secondary Organic Aerosol (IEPOX-SOA) from aerosol mass spectrometer measurements, Atmos. Chem. Phys. Discuss., 15, 11223–11276, doi:10.5194/acpd-15-11223-2015, 2015.

Huie, R. E. and Herron, J. T.: Kinetics of the reactions of singlet molecular oxygen $(O_2^1\Delta_g)$ with organic compounds in the gas phase, Int. J. Chem. Kinet., 5, 197–211, doi:10.1002/kin.550050204, 1973.

Jathar, S. H., Cappa, C. D., Wexler, A. S., Seinfeld, J. H., and Kleeman, M. J.: Multi-generational oxidation model to simulate secondary organic aerosol in a 3-D air quality model, Geosci. Model Dev., 8, 2553–2567, doi:10.5194/gmd-8-2553-2015, 2015.

Johnson, M. S., Nilsson, E. J. K., Svensson, E. A., and Langer, S.: Gas-phase advanced oxidation for effective, efficient in situ control of pollution., Environ. Sci. Technol., 48, 8768–8776, doi:10.1021/es5012687, 2014.

Kang, E., Root, M. J., Toohey, D. W., and Brune, W. H.: Introducing the concept of Potential Aerosol Mass (PAM), Atmos. Chem. Phys., 7, 5727–5744, doi:10.5194/acp-7-5727-2007, 2007.

Kang, E., Toohey, D. W., and Brune, W. H.: Dependence of SOA oxidation on organic aerosol mass concentration and OH exposure: experimental PAM chamber studies, Atmos. Chem. Phys., 11, 1837–1852, doi:10.5194/acp-11-1837-2011, 2011.

Klems, J. P., Lippa, K. A., and McGivern, W. S.: Quantitative evidence for organic peroxy radical photochemistry at 254 nm, J. Phys. Chem. A, 119, 344–351, doi:10.1021/jp509165x, 2015.

Lambe, A. T., Ahern, A. T., Williams, L. R., Slowik, J. G., Wong, J. P. S., Abbatt, J. P. D., Brune, W. H., Ng, N. L., Wright, J. P., Croasdale, D. R., Worsnop, D. R., Davidovits, P., and Onasch, T. B.: Characterization of aerosol photooxidation flow reactors: heterogeneous oxidation, secondary organic aerosol formation and cloud condensation nuclei activity measurements, Atmos. Meas. Tech., 4, 445–461, doi:10.5194/amt-4-445-2011, 2011a.

Lambe, A. T., Onasch, T. B., Massoli, P., Croasdale, D. R., Wright, J. P., Ahern, A. T., Williams, L. R., Worsnop, D. R., Brune, W. H., and Davidovits, P.: Laboratory studies of the chemical composition and cloud condensation nuclei (CCN) activity of secondary or-

ganic aerosol (SOA) and oxidized primary organic aerosol (OPOA), Atmos. Chem. Phys., 11, 8913–8928, doi:10.5194/acp-11-8913-2011, 2011b.

Lambe, A. T., Onasch, T. B., Croasdale, D. R., Wright, J. P., Martin, A. T., Franklin, J. P., Massoli, P., Kroll, J. H., Canagaratna, M. R., Brune, W. H., Worsnop, D. R., and Davidovits, P.: Transitions from functionalization to fragmentation reactions of laboratory secondary organic aerosol (SOA) generated from the OH oxidation of alkane precursors, Environ. Sci. Technol., 46, 5430–5437, doi:10.1021/es300274t, 2012.

Lambe, A. T., Cappa, C. D., Massoli, P., Onasch, T. B., Forestieri, S. D., Martin, A. T., Cummings, M. J., Croasdale, D. R., Brune, W. H., Worsnop, D. R., and Davidovits, P.: Relationship between oxidation level and optical properties of secondary organic aerosol, Environ. Sci. Technol., 47, 6349–6357, doi:10.1021/es401043j, 2013.

Lambe, A. T., Chhabra, P. S., Onasch, T. B., Brune, W. H., Hunter, J. F., Kroll, J. H., Cummings, M. J., Brogan, J. F., Parmar, Y., Worsnop, D. R., Kolb, C. E., and Davidovits, P.: Effect of oxidant concentration, exposure time, and seed particles on secondary organic aerosol chemical composition and yield, Atmos. Chem. Phys., 15, 3063–3075, doi:10.5194/acp-15-3063-2015, 2015.

Laue, T. and Plagens, A.: Named Organic Reactions, 2nd edn., John Wiley & Sons, Chichester, England, New York, USA, available at: http://www.wiley.com/WileyCDA/WileyTitle/productCd-047001041X.html (last access: July 2015), 2005.

Levy II., H.: Normal atmosphere: large radical and formaldehyde concentrations predicted, Science, 173, 141–143, doi:10.1126/science.173.3992.141, 1971.

Li, R., Palm, B. B., Borbon, A., Graus, M., Warneke, C., Ortega, A. M., Day, D. A., Brune, W. H., Jimenez, J. L., and de Gouw, J. A.: Laboratory studies on secondary organic aerosol formation from crude oil vapors, Environ. Sci. Technol., 47, 12566–12574, doi:10.1021/es402265y, 2013.

Li, R., Palm, B. B., Ortega, A. M., Hu, W., Peng, Z., Day, D. A., Knote, C., Brune, W. H., de Gouw, J., and Jimenez, J. L.: Modeling the radical chemistry in an Oxidation Flow Reactor (OFR): radical formation and recycling, sensitivities, and OH exposure estimation equation, J. Phys. Chem. A, 119, 4418–4432, doi:10.1021/jp509534k, 2015.

Liu, P. F., Abdelmalki, N., Hung, H.-M., Wang, Y., Brune, W. H., and Martin, S. T.: Ultraviolet and visible complex refractive indices of secondary organic material produced by photooxidation of the aromatic compounds toluene and *m*-xylene, Atmos. Chem. Phys., 15, 1435–1446, doi:10.5194/acp-15-1435-2015, 2015.

Title Page

Abstract | Introduction

Conclusions | References

Tables | Figures

|◄ | ►|

◄ | ►

Back | Close

Full Screen / Esc

Printer-friendly Version

Interactive Discussion

Mao, J., Ren, X., Brune, W. H., Olson, J. R., Crawford, J. H., Fried, A., Huey, L. G., Cohen, R. C., Heikes, B., Singh, H. B., Blake, D. R., Sachse, G. W., Diskin, G. S., Hall, S. R., and Shetter, R. E.: Airborne measurement of OH reactivity during INTEX-B, Atmos. Chem. Phys., 9, 163–173, doi:10.5194/acp-9-163-2009, 2009.

5 Massoli, P., Lambe, A. T., Ahern, A. T., Williams, L. R., Ehn, M., Mikkilä, J., Canagaratna, M. R., Brune, W. H., Onasch, T. B., Jayne, J. T., Petäjä, T., Kulmala, M., Laaksonen, A., Kolb, C. E., Davidovits, P., and Worsnop, D. R.: Relationship between aerosol oxidation level and hygroscopic properties of laboratory generated secondary organic aerosol (SOA) particles, Geophys. Res. Lett., 37, L24801, doi:10.1029/2010GL045258, 2010.

10 Matsunaga, A. and Ziemann, P. J.: Gas-wall partitioning of organic compounds in a Teflon film chamber and potential effects on reaction product and aerosol yield measurements, Aerosol Sci. Tech., 44, 881–892, doi:10.1080/02786826.2010.501044, 2010.

Monks, P. S.: Gas-phase radical chemistry in the troposphere, Chem. Soc. Rev., 34, 376–395, doi:10.1039/b307982c, 2005.

15 Nakashima, N.: Laser photolysis of benzene. V. Formation of hot benzene, J. Chem. Phys., 77, 6040, doi:10.1063/1.443847, 1982.

Nakashima, N. and Yoshihara, K.: Laser flash photolysis of benzene. VIII. Formation of hot benzene from the S_2 state and its collisional deactivation, J. Chem. Phys., 79, 2727–2735, doi:10.1063/1.446176, 1983.

20 Nguyen, T. B., Crounse, J. D., Schwantes, R. H., Teng, A. P., Bates, K. H., Zhang, X., St. Clair, J. M., Brune, W. H., Tyndall, G. S., Keutsch, F. N., Seinfeld, J. H., and Wennberg, P. O.: Overview of the Focused Isoprene eXperiment at the California Institute of Technology (FIXCIT): mechanistic chamber studies on the oxidation of biogenic compounds, Atmos. Chem. Phys., 14, 13531–13549, doi:10.5194/acp-14-13531-2014, 2014.

25 Odum, J. R., Hoffmann, T., Bowman, F., Collins, D., Flagan Richard, C., and Seinfeld John, H.: Gas particle partitioning and secondary organic aerosol yields, Environ. Sci. Technol., 30, 2580–2585, doi:10.1021/es950943+, 1996.

Ono, R., Nakagawa, Y., Tokumitsu, Y., Matsumoto, H., and Oda, T.: Effect of humidity on the production of ozone and other radicals by low-pressure mercury lamps, J. Photoch. Photobio. A, 274, 13–19, doi:10.1016/j.jphotochem.2013.09.012, 2014.

30 Ortega, A. M., Day, D. A., Cubison, M. J., Brune, W. H., Bon, D., de Gouw, J. A., and Jimenez, J. L.: Secondary organic aerosol formation and primary organic aerosol oxida-

tion from biomass-burning smoke in a flow reactor during FLAME-3, Atmos. Chem. Phys., 13, 11551–11571, doi:10.5194/acp-13-11551-2013, 2013.

Ortega, A. M., Hayes, P. L., Peng, Z., Palm, B. B., Hu, W., Day, D. A., Li, R., Cubison, M. J., Brune, W. H., Graus, M., Warneke, C., Gilman, J. B., Kuster, W. C., de Gouw, J. A., and Jimenez, J. L.: Real-time measurements of secondary organic aerosol formation and aging from ambient air in an oxidation flow reactor in the Los Angeles area, Atmos. Chem. Phys. Discuss., 15, 21907–21958, doi:10.5194/acpd-15-21907-2015, 2015.

Palm, B. B., Campuzano-Jost, P., Ortega, A. M., Day, D. A., Karl, T., Kaser, L., Jud, W., Hansel, A., Fry, J. L., Brown, S. S., Zarzana, K. J., Dube, W. P., Wagner, N. L., Draper, D. C., Hunter, J. F., Kroll, J. H., Brune, W. H., and Jimenez, J. L.: Real-time organic aerosol formation and oxidative aging using a flow reactor in a pine forest, in preparation, 2015.

Peng, Z., Day, D. A., Stark, H., Li, R., Palm, B. B., Brune, W. H., and Jimenez, J. L.: HO_x radical chemistry in oxidation flow reactors with low-pressure mercury lamps systematically examined by modeling, Atmos. Meas. Tech. Discuss., 8, 3883–3932, doi:10.5194/amtd-8-3883-2015, 2015.

Platt, S. M., El Haddad, I., Zardini, A. A., Clairotte, M., Astorga, C., Wolf, R., Slowik, J. G., Temime-Roussel, B., Marchand, N., Ježek, I., Drinovec, L., Močnik, G., Möhler, O., Richter, R., Barmet, P., Bianchi, F., Baltensperger, U., and Prévôt, A. S. H.: Secondary organic aerosol formation from gasoline vehicle emissions in a new mobile environmental reaction chamber, Atmos. Chem. Phys., 13, 9141–9158, doi:10.5194/acp-13-9141-2013, 2013.

Presto, A. A., Huff Hartz, K. E., and Donahue, N. M.: Secondary organic aerosol production from terpene ozonolysis. 1. Effect of UV radiation, Environ. Sci. Technol., 39, 7036–7045, doi:10.1021/es050174m, 2005.

Renlund, A. M. and Trott, W. M.: ArF Laser-induced decomposition of simple energetic niolecules, Chem. Phys. Lett., 107, 555–560, doi:10.1016/S0009-2614(84)85155-6, 1984.

Roberts, J. M. and Fajer, R. W.: UV absorption cross sections of organic nitrates of potential atmospheric importance and estimation of atmospheric lifetimes, Environ. Sci. Technol., 23, 945–951, 1989.

Romonosky, D. E., Laskin, A., Laskin, J., and Nizkorodov, S. A.: High-resolution mass spectrometry and molecular characterization of aqueous photochemistry products of common types of secondary organic aerosols, J. Phys. Chem. A, 119, 2594–2606, doi:10.1021/jp509476r, 2015.

Sander, S. P., Friedl, R. R., Barker, J. R., Golden, D. M., Kurylo, M. J., Wine, P. H., Abbatt, J. P. D., Burkholder, J. B., Kolb, C. E., Moortgat, G. K., Huie, R. E., and Orkin, V. L.: Chemical Kinetics and Photochemical Data for Use in Atmospheric Studies Evaluation Number 17, available at: http://jpldataeval.jpl.nasa.gov/pdf/JPL%20 10-6 %20 Final%20 15June2011.pdf (last access: July 2015), 2011.

Saukko, E., Lambe, A. T., Massoli, P., Koop, T., Wright, J. P., Croasdale, D. R., Pedernera, D. A., Onasch, T. B., Laaksonen, A., Davidovits, P., Worsnop, D. R., and Virtanen, A.: Humidity-dependent phase state of SOA particles from biogenic and anthropogenic precursors, Atmos. Chem. Phys., 12, 7517–7529, doi:10.5194/acp-12-7517-2012, 2012.

Schmidt, G. A., Kelley, M., Nazarenko, L., Ruedy, R., Russell, G. L., Aleinov, I., Bauer, M., Bauer, S. E., Bhat, M. K., Bleck, R., Canuto, V., Chen, Y., Cheng, Y., Clune, T. L., Del Genio, A., de Fainchtein, R., Faluvegi, G., Hansen, J. E., Healy, R. J., Kiang, N. Y., Koch, D., Lacis, A. A., LeGrande, A. N., Lerner, J., Lo, K. K., Matthews, E. E., Menon, S., Miller, R. L., Oinas, V., Oloso, A. O., Perlwitz, J. P., Puma, M. J., Putman, W. M., Rind, D., Romanou, A., Sato, M., Shindell, D. T., Sun, S., Syed, R. A., Tausnev, N., Tsigaridis, K., Unger, N., Voulgarakis, A., Yao, M.-S., and Zhang, J.: Configuration and assessment of the GISS ModelE2 contributions to the CMIP5 archive, J. Adv. Model. Earth Syst., 6, 141–184, doi:10.1002/2013MS000265, 2014.

Seakins, P. W.: A brief review of the use of environmental chambers for gas phase studies of kinetics, chemical mechanisms and characterisation of field instruments, EPJ Web Conf., 9, 143–163, doi:10.1051/epjconf/201009012, 2010.

Smith, J. D., Kroll, J. H., Cappa, C. D., Che, D. L., Liu, C. L., Ahmed, M., Leone, S. R., Worsnop, D. R., and Wilson, K. R.: The heterogeneous reaction of hydroxyl radicals with sub-micron squalane particles: a model system for understanding the oxidative aging of ambient aerosols, Atmos. Chem. Phys., 9, 3209–3222, doi:10.5194/acp-9-3209-2009, 2009.

Tkacik, D. S., Lambe, A. T., Jathar, S., Li, X., Presto, A. A., Zhao, Y., Blake, D., Meinardi, S., Jayne, J. T., Croteau, P. L., and Robinson, A. L.: Secondary organic aerosol formation from in-use motor vehicle emissions using a potential aerosol mass reactor, Environ. Sci. Technol., 48, 11235–11242, doi:10.1021/es502239v, 2014.

Tsang, W.: Chemical kinetic data base for combustion chemistry Part V. Propene, J. Phys. Chem. Ref. Data, 20, 221–274, doi:10.1063/1.555880, 1991.

Wang, B., Lambe, A. T., Massoli, P., Onasch, T. B., Davidovits, P., Worsnop, D. R., and Knopf, D. A.: The deposition ice nucleation and immersion freezing potential of amorphous

Non-OH chemistry in oxidation flow reactors

Z. Peng et al.

Title Page

Abstract | Introduction

Conclusions | References

Tables | Figures

|◄ | ►|

◄ | ►

Back | Close

Full Screen / Esc

Printer-friendly Version

Interactive Discussion

secondary organic aerosol: pathways for ice and mixed-phase cloud formation, J. Geophys. Res., 117, D16209, doi:10.1029/2012JD018063, 2012.

Wang, J., Doussin, J. F., Perrier, S., Perraudin, E., Katrib, Y., Pangui, E., and Picquet-Varrault, B.: Design of a new multi-phase experimental simulation chamber for atmospheric photosmog, aerosol and cloud chemistry research, Atmos. Meas. Tech., 4, 2465–2494, doi:10.5194/amt-4-2465-2011, 2011.

Warneke, C., Roberts, J. M., Veres, P., Gilman, J., Kuster, W. C., Burling, I., Yokelson, R., and de Gouw, J. A.: VOC identification and inter-comparison from laboratory biomass burning using PTR-MS and PIT-MS, Int. J. Mass Spectrom., 303, 6–14, doi:10.1016/j.ijms.2010.12.002, 2011.

Wong, J. P. S., Zhou, S., and Abbatt, J. P. D.: Changes in secondary organic aerosol composition and mass due to photolysis: relative humidity dependence, J. Phys. Chem. A, 119, 4309–4316, doi:10.1021/jp506898c, 2015.

Zhang, X., Cappa, C. D., Jathar, S. H., McVay, R. C., Ensberg, J. J., Kleeman, M. J., and Seinfeld, J. H.: Influence of vapor wall loss in laboratory chambers on yields of secondary organic aerosol, P. Natl. Acad. Sci. USA, 111, 5802–5807, doi:10.1073/pnas.1404727111, 2014.

Non-OH chemistry in oxidation flow reactors

Z. Peng et al.

Title Page

Abstract | Introduction

Conclusions | References

Tables | Figures

Back | Close

Full Screen / Esc

Printer-friendly Version

Interactive Discussion

Table 1. Code of the labels of typical cases. A case label is composed of three characters denoting the water mixing ratio, the photon flux, and the external OH reactivity, respectively.

	Water mixing ratio	Photon flux	External OH reactivity
Options	L = low (0.07 %)	L = low (10^{11} photons cm^{-2} s^{-1} at 185 nm; 4.17 × 10^{13} photons cm^{-2} s^{-1} at 254 nm)	0
	M = medium (1 %)	M = medium (10^{13} photons cm^{-2} s^{-1} at 185 nm; 1.45 × 10^{15} photons cm^{-2} s^{-1} at 254 nm)	L = low (10 s^{-1}) typically for remote or clean urban air
	H = high (2.3 %)	H = high (10^{14} photons cm^{-2} s^{-1} at 185 nm; 8.51 × 10^{15} photons cm^{-2} s^{-1} at 254 nm)	H = high (100 s^{-1}) typically for polluted urban air
		"L" = lowest in Li et al. (2015)'s PAM (7.9 × 10^{11} photons cm^{-2} s^{-1} at 185 nm; 2.04 × 10^{14} photons cm^{-2} s^{-1} at 254 nm)	V = very high (1000 s^{-1}) only for laboratory experiments
Example	LH0:	low water mixing ratio, high photon flux, no external OH reactivity	

Figure 1. Fractional importance of the photolysis rate at 185 nm of several species of interest vs. the reaction rate with OH, as a function of the ratio of exposure to 185 nm photons (F185) and OH. The modeled range for OFR185 and for pathological conditions for OFR185 are also shown. The curves of aromatics and inorganic gases are highlighted by solid dots and upward triangles, respectively. The lower inset shows histograms of model-estimated F185/OH exposures for three field studies where OFR185 was used to process ambient air. The upper inset (black and blue markers) shows the same information for source studies of biomass smoke (FLAME-3; Ortega et al., 2013) and an urban tunnel (Tkacik et al., 2014). All curves, markers, and histograms share the same abscissa.
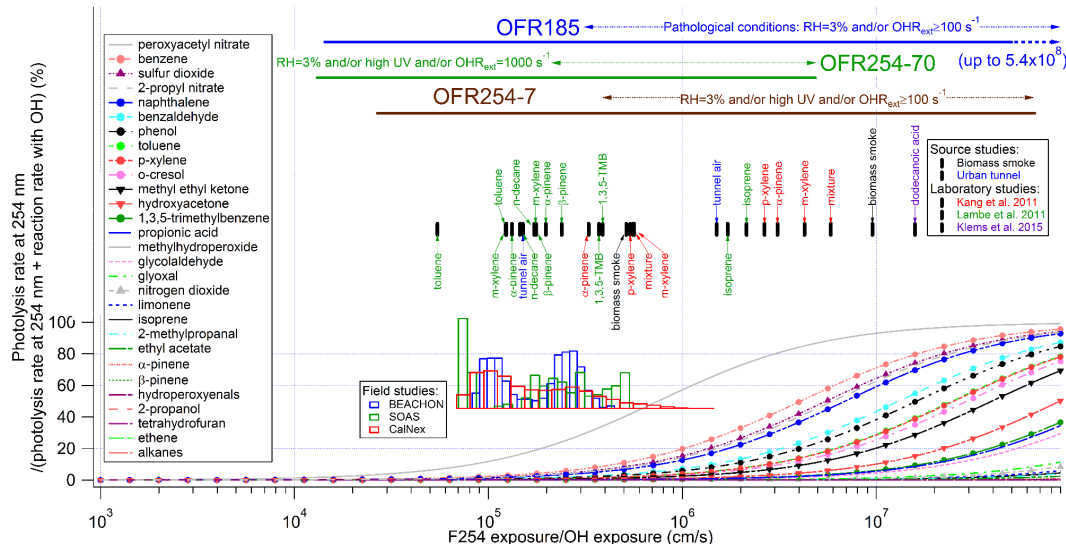
Figure 2. Same format as Fig. 1, but for the fractional importance of the photolysis rate at 254 nm vs. the reaction rate with OH as a function of the ratio of exposure to 254 nm (F254) and OH. The modeled range for OFR254-70 and OFR254-7 and for corresponding pathological conditions are also shown. The curves of ketones are highlighted by downward triangles. The insets show histograms of model-estimated F254/OH exposures for three field studies where OFR185 was used to process ambient air. In addition to source studies of biomass smoke (FLAME-3) and urban tunnel (Tkacik et al., 2014), F254 exposure/OH exposure ratios in two laboratory studies (Kang et al., 2011; Lambe et al., 2011b) are shown in the upper inset. Colored tags indicate species used in the laboratory experiments. The lower and upper limits of F254 exposure/OH exposure ratios in the experiments with a certain source in a certain study are denoted by tags below and above the markers, respectively.
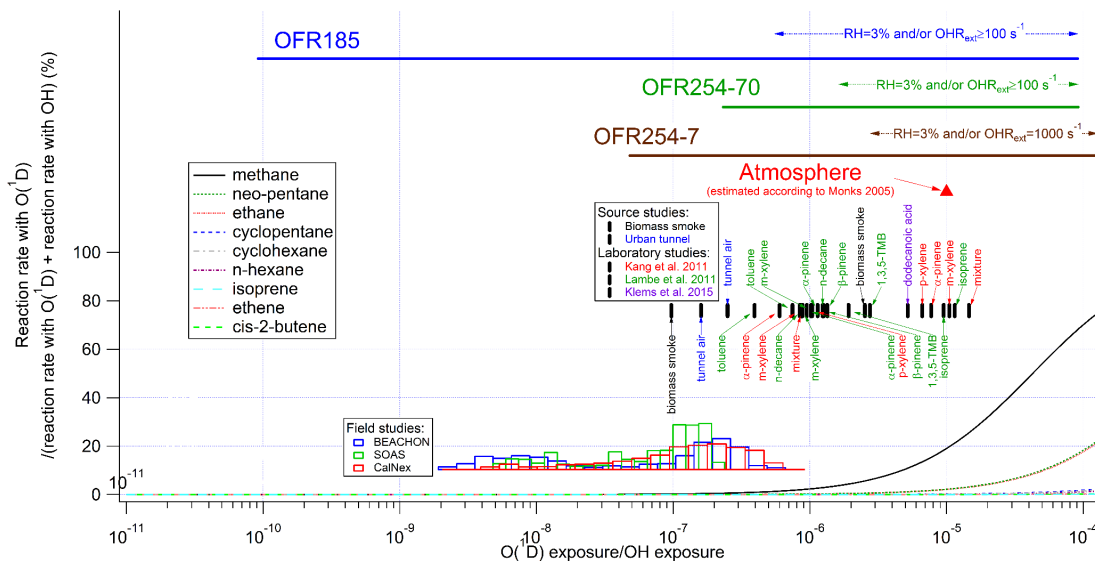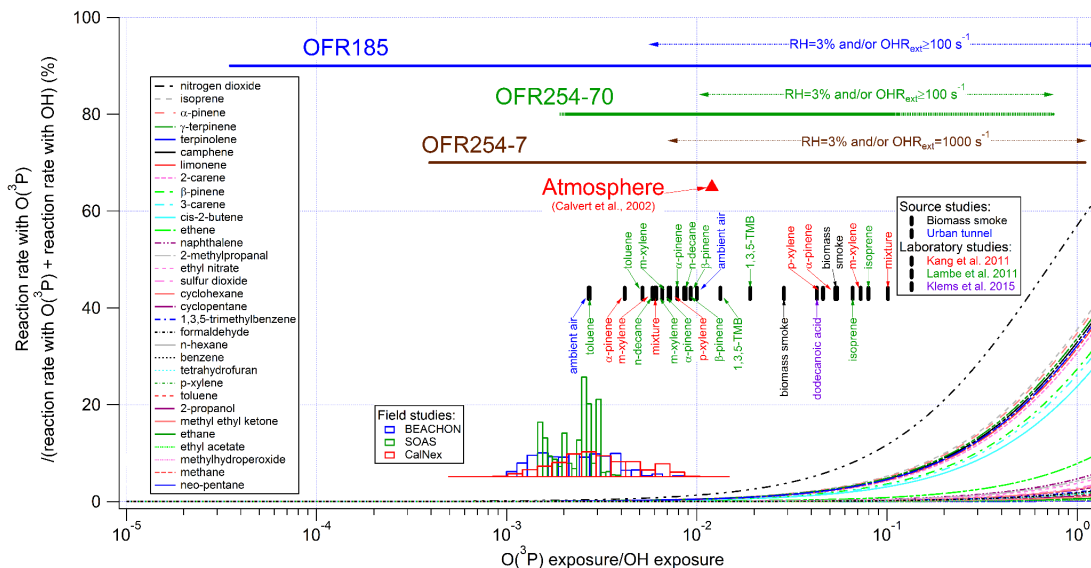
Figure 3. Same format as Fig. 2, but for the ratio of the reaction rate with $O(^1D)$ vs. OH as a function of the relative exposure to $O(^1D)$ and OH. A typical value of the relative exposure of $O(^1D)$ and OH in the troposphere estimated according to Monks (2005) is also shown.

Figure 4. Same format as Fig. 3, but for the ratio of the reaction rate with $O(^3P)$ vs. OH as a function of the relative exposure of $O(^3P)$ and OH. A typical value of the relative exposure of $O(^3P)$ and OH in the troposphere from Calvert et al. (2002) is also shown.
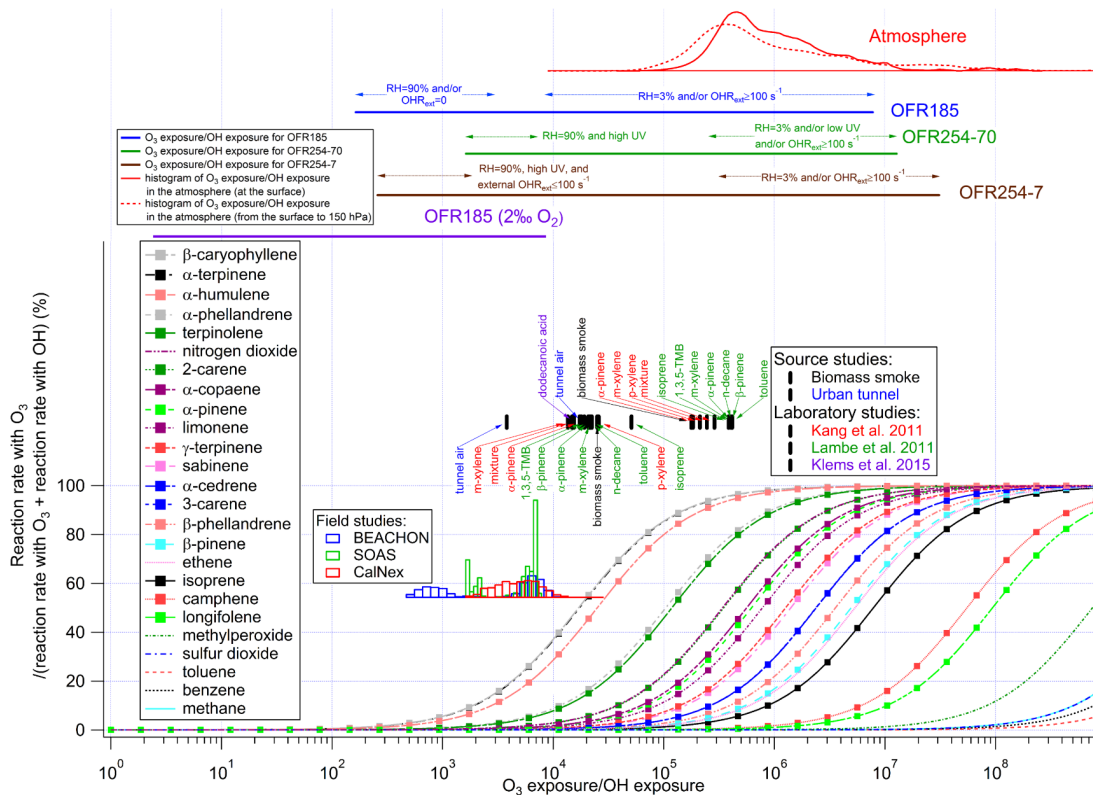
Figure 5. Same format as Fig. 2, but for the fractional importance of the reaction rate with O_3 vs. OH as a function of the relative exposure of O_3 and OH. The curves of biogenics are highlighted by squares. Also shown are modeled distributions of the relative exposure of O_3 and OH at the Earth's surface (solid line) and throughout the column from the surface to a height with a pressure of 150 hPa (dashed line). The distributions were calculated from the mean daily concentrations of O_3 and OH as simulated by the GISS ModelE2.

Title Page

Abstract | Introduction

Conclusions | References

Tables | Figures

|◀ | ▶|

◀ | ▶

Back | Close

Full Screen / Esc

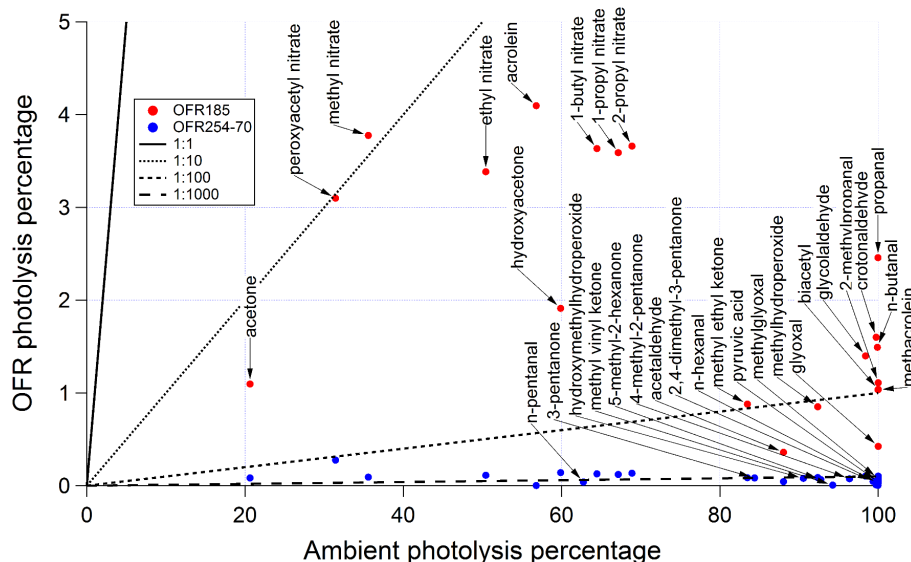Printer-friendly Version

Interactive Discussion

Figure 6. Ambient photolysis percentages of secondary species in a week (calculated from photolysis rates reported in Hodzic et al., 2015) vs. photolysis percentages of those species in OFR185 and OFR254-70 reaching the same photochemical age (ambient OH concentration of 1.5×10^6 molecules cm^{-3} assumed) under the condition of 70 % relative humidity and 25 s^{-1} initial OHR$_{ext}$. If the points of a certain species for both OFR185 and OFR254-70 are available, the species name is tagged on the OFR185 point, otherwise on the OFR254-70 point. The 1 : 1, 1 : 10, 1 : 100, and 1 : 1000 lines are also shown for comparison.
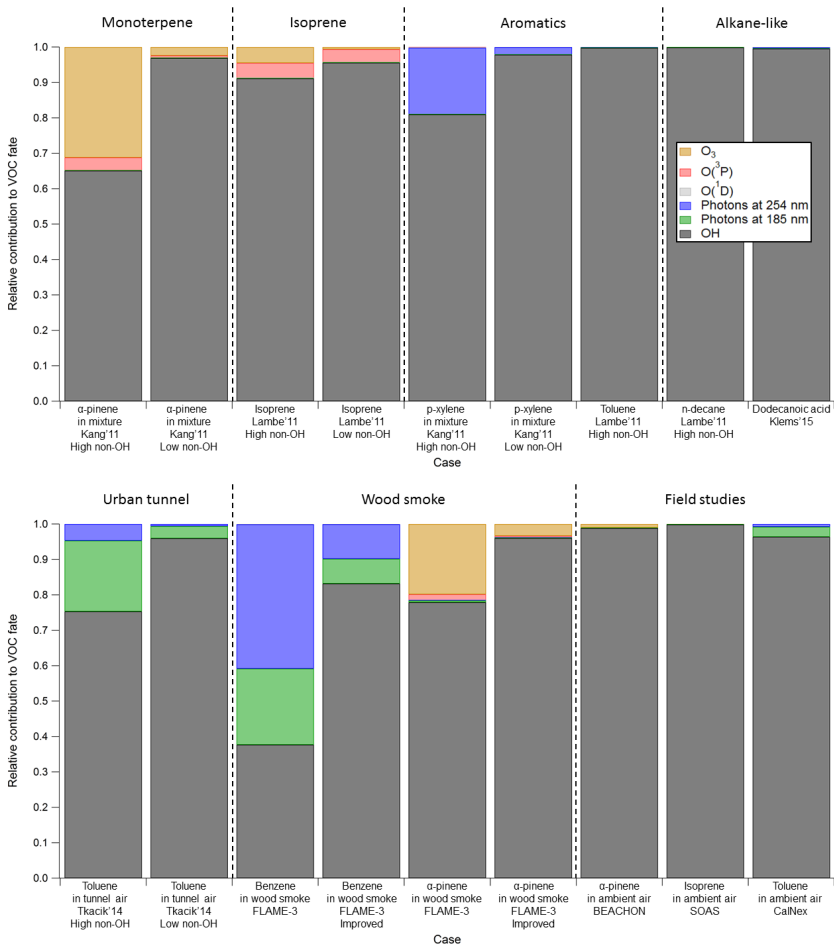
Figure 7. VOC fate in several representative cases of the laboratory, source, and field studies examined in this work. More details on VOC fate in these studies can be found in Table S4.

Title Page

Abstract | Introduction

Conclusions | References

Tables | Figures

|◄ | ►|

◄ | ►

Back | Close

Full Screen / Esc

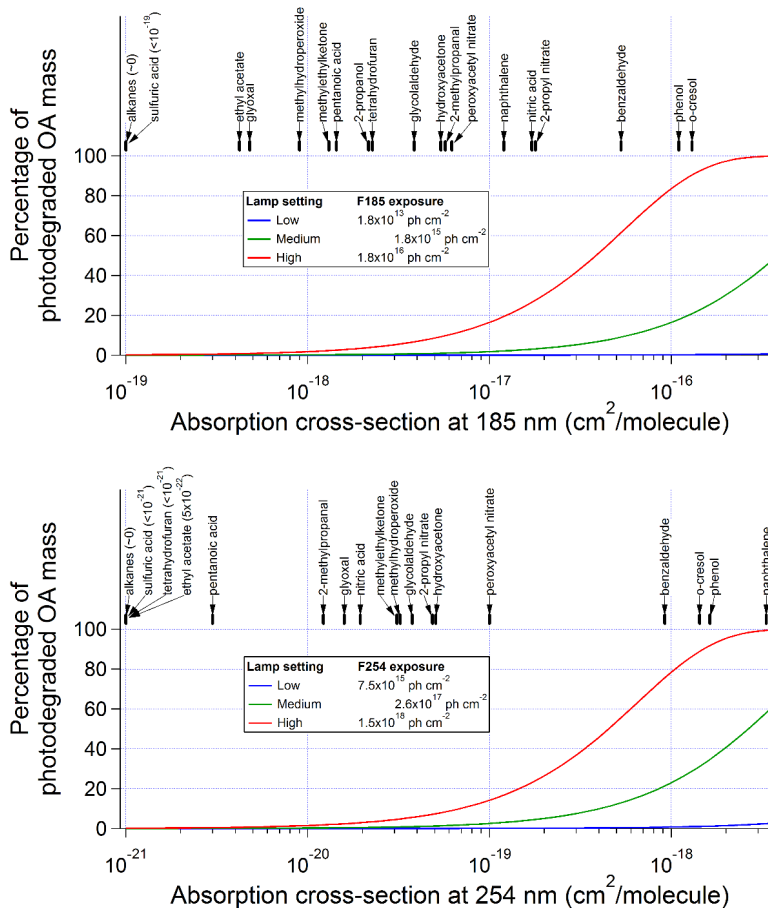Printer-friendly Version

Interactive Discussion

Figure 8. Percentage of SOA photodegradation at (upper) 185 and (lower) 254 nm at different UV levels as a function of absorption cross-section under the assumption of unity quantum yield. Absorption cross-sections of some representative SOA components are also shown.

Title Page

Abstract | Introduction

Conclusions | References

Tables | Figures

|◀ | ▶|

◀ | ▶

Back | Close

Full Screen / Esc

Printer-friendly Version

Interactive Discussion